CONTACT MELTING OF A THREE-DIMENSIONAL PHASE CHANGE MATERIAL ON A FLAT SUBSTRATE

MICHELLE M. DE DECKER AND TIM G. MYERS

Abstract. In this paper a model is developed to describe the three dimensional contact melting process of a cuboid on a heated surface. The mathematical description involves two heat equations (one in the solid and one in the melt), the Navier-Stokes equations for the flow in the melt, a Stefan condition at the phase change interface and a force balance between the weight of the solid and the countering pressure in the melt. In the solid an optimised heat balance integral method is used to approximate the temperature. In the liquid the small aspect ratio allows the Navier-Stokes and heat equations to be simplified considerably so that the liquid pressure may be determined using an eigenfunction expansion and finally the problem is reduced to solving three first order ordinary differential equations. Results are presented showing the evolution of the melting process. Further reductions to the system are made to provide simple guidelines concerning the process. Comparison of the solutions with experimental data on the melting of n-octadecane shows excellent agreement.

1. Introduction

Contact melting is the process whereby a phase change material (PCM) is placed on a surface that is maintained above the phase change temperature. The heat from the surface causes the PCM to melt and it then rests on its own melt layer. The process may be easily observed by placing a piece of ice on a warm surface: after a short time the ice will sit on a thin layer of water as it slowly melts. Dropping water into a hot frying pan results in the water floating on a vapour layer (the Leidenfrost effect), see [1, 15]. Industrially the process is exploited in thermal storage systems where energy is stored in the form of latent heat which is released upon melting [2, 6].

During the contact melting process the melt layer that forms between the solid and substrate is subject to the weight of the solid and this induces a flow. The fluid layer remains thin since fluid is constantly being forced out from under the solid. Consequently the solid is always close to the substrate and so the melting process is relatively rapid. Typically the thickness of the melted material is proportional to time (this will be discussed in detail later). This may be

Key words and phrases. Contact melting; Stefan problems; Phase change; Lubrication theory; Heat Balance Integral Method.

contrasted to the standard one-dimensional Stefan problem, where weight is neglected, and the thickness is proportional to $\sqrt{t}$. For this reason contact melting, rather than melting a fixed solid, is exploited in thermal storage systems.

To describe the contact-melting process mathematically an account of the heat flow in the solid and liquid layers and the fluid flow is required. Clearly the thickness of the solid layer decreases with time and depends on the melt rate. The behaviour of the liquid layer is not so obvious since it depends on the melt rate and flow, which is driven by the decreasing weight of the solid. In the past the complexity of the mathematical model, coupling heat equations and the Navier-Stokes equation over unknown domains, forced many simplifications on the analysis. Typical assumptions include:

(1) The temperature of the solid remains at the melting temperature, T_m, throughout the process.
(2) The melting process is in a quasi-steady state, that is, if the position of the melt front is denoted $h(t)$ then $h_t = 0$.
(3) Heat transfer in the liquid is dominated by conduction across the film.
(4) The lubrication approximation holds in the liquid layer, so the flow is primarily parallel to the solid surface and driven by the pressure gradient. The pressure variation across the film is negligible.
(5) The amount of melted fluid is small compared to that of the initial solid.
(6) There is perfect thermal contact between the liquid and substrate or there is a constant heat flux.
(7) The problem is two-dimensional,

see [2, 5, 6, 7, 16].

Recently Myers *et al.* [16] developed a two-dimensional model where assumptions 1,2,5,6 were removed whilst assumptions 3,4 were shown to lead to small errors. Comparison of the results of this model with experimental data from Moallemi *et al.* [10] showed excellent agreement. However, in order to obtain this agreement a high heat transfer coefficient (HTC) was required. A possible explanation for this high value comes from the fact that the model was two-dimensional. If the substrate is defined by the $x - y$ plane then the two-dimensional model only allows fluid to move in the x direction and escape at the sides of the block defined by $x = \pm L$. In reality the fluid in the experiments of [10] could also flow in the y direction and escape at the sides defined by $y = \pm W$. This additional escape route would obviously result in a thinner fluid layer which in turn would require a lower heat transfer coefficient to provide the same melt rate as a two-dimensional model. This observation provides the motivation for the current study where we detail the three-dimensional extension to the model described in [16].

Previous three-dimensional mathematical analyses of contact melting may be found in the papers by Lacroix [8] and Yoo [18]. Lacroix uses a model that

incorporates a varying mass and temperature within the solid, so removing assumptions 1, 2, 5. However, there are a number of inconsistencies in the model (described in detail in [16]). In particular, when calculating the temperature in the solid the method of separation of variables is used. Unfortunately, since the domain of interest is changing the 'constant of separation' is time dependent and so the solution is invalid. Yoo deals with a constant mass, isothermal solid but permits non-steady motion, so removing assumption 2. His solution is primarily aimed at improving understanding of the small time behaviour, typically in the first 15s. Within the context of the applied assumptions his solution is correct and so in the latter sections of the paper we will use the results of Yoo for comparison, but stress that we expect them to become less accurate with increasing time.

The experimental work of Moallemi *et al.* [10] involved a three-dimensional solid block, insulated at the sides and top. Although they attempt to make the physical situation close to two-dimensional by using a block with a large aspect ratio base (the ratio of the length to the width is 6) it is still clearly a three-dimensional experiment and so we will also compare our model with their data.

In the following sections we first develop the three-dimensional model and the appropriate simplifications. In the fluid layer we will exploit the small aspect ratio to reduce the Navier-Stokes equations via lubrication theory. Similarly the heat equation will be shown to reduce to a simple quasi-steady form, that is, time drops out of the equation but remains in the boundary condition. In the solid the full heat equation holds. Key to this analysis is the assumption that the temperature of the substrate does not vary in space. This then leads to a flat interface at the base of the PCM for all time and, since the temperature there is the constant melt temperature, the result is that the solid temperature only varies in the direction perpendicular to the interface. This permits us to use a heat balance integral method, as described in [11, 12]. In §4 we compare our results with the analytical solution of Yoo [18] and the experimental data provided in [10] to show that the new three-dimensional model also provides excellent agreement, but with a heat transfer coefficient less than half that of the two-dimensional analysis. Finally, we use the knowledge gained from solving the three-dimensional model to reduce the system further: firstly, two first order ordinary differential equations and secondly, an even simpler model where the solid height decreases linearly with time.

2. Mathematical model

In line with the experiments of Moallemi *et al.* [10] we model a PCM that is cuboid and placed on a flat surface. The top and sides are insulated: this feature is key to the mathematical model. Since heat is gained only through the bottom of the block and during the melting process the bottom is at the constant phase change temperature the heat transfer occurs only in the direction perpendicular

to the bottom. Initially the block has dimensions $2L \times 2W \times H$, so the width is described along $x \in [-L, L]$, the breadth $y \in [-W, W]$ and the height $z \in [0, H]$. The problem configuration is depicted in Fig. 1.

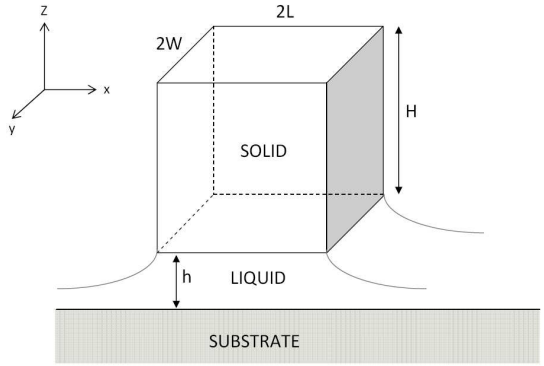

FIGURE 1. Problem configuration: Cuboid PCM floating on a liquid layer

Following [16] we may split the melting process into 3 stages. The first stage is the pre-melt stage, which occurs from the time the cuboid comes into contact with the heated surface until the bottom of the block reaches the melting temperature, T_m, and melting begins. This first stage is typically short and occurs for $t \in [0, t_1]$ where t_1 is determined by setting the temperature at $z = 0$ to T_m. The second stage is that in which the liquid layer is first formed and the block begins to float upon it. This stage occurs for $t \in [t_1, t_2]$ and ends when the temperature at the top of the solid rises (noticeably) above the initial temperature, denoted θ_0. So t_2 is the time at which the temperature at the top of the block first exceeds θ_0 (according to the mathematical model). Finally, stage 3 begins at t_2 and ends once all the block is melted, i.e. $t \in [t_2, t_m]$. Note, the distinction between stages 2 and 3 is a requirement of the mathematical model and a different approach may not require this.

The height of the liquid layer is denoted by $h(t)$ and it occupies $z \in [0, h]$. The solid height is denoted $H(t)$ and initially $H(0) = H_0$. We define the height of melted solid, $h_m(t)$, through the relation $H(t) = H_0 - h_m(t)$. The mass of the solid is then $M(t) = 4\rho_s LW[H_0 - h_m]$.

In order to solve the fluid flow equations we exploit the thinness of the layer and so impose the lubrication approximation:

$$\eta \frac{\partial^2 u}{\partial z^2} = \frac{\partial p}{\partial x}, \qquad \eta \frac{\partial^2 v}{\partial z^2} = \frac{\partial p}{\partial y}, \qquad \frac{\partial p}{\partial z} = 0, \tag{1}$$

where η is the viscosity, the velocity vector is given by $\vec{u}_l = (u, v, w)$ for the x, y, z directions respectively and p is the pressure. The largest term that has been neglected is $\mathcal{O}(\epsilon^2 Re)$ where, if $\mathcal{H}$ is the height scale and $\mathcal{L}$ the length scale

(in general $\mathcal{L} = L$), then $\epsilon = \mathcal{H}/\mathcal{L}$ and $\epsilon^2 Re$ is the reduced Reynolds number [17]. The flow is incompressible so the continuity equation is

$$\frac{\partial u}{\partial x} + \frac{\partial v}{\partial y} + \frac{\partial w}{\partial z} = 0. \tag{2}$$

At the substrate, $z = 0$, we prescribe the standard no slip condition

$$u = v = w = 0, \tag{3}$$

and at the top of the liquid layer, $z = h$, there is no slip in the x and y direction,

$$u = v = 0. \tag{4}$$

The pressure is ambient at the edge of the block,

$$p|_{x=\pm L} = p|_{y=\pm W} = 0. \tag{5}$$

The final condition required to solve the flow equations is derived from a momentum balance at $z = h$

$$\rho_s \vec{n} \cdot (\vec{u_s} - \vec{u_b}) = \rho_l \vec{n} \cdot (\vec{u_l} - \vec{u_b}), \tag{6}$$

where $\vec{u_s}$, $\vec{u_l}$ and $\vec{u_b}$ are the velocity vectors in the solid, liquid and boundary respectively and $\vec{n}$ is the normal vector at the solid-liquid interface, see [13]. In our case these are

$$\vec{n} = (0, 0, 1), \quad \vec{u_s} = (0, 0, h_t - h_{mt}), \quad \vec{u_l} = (u, v, w), \quad \vec{u_b} = (0, 0, h_t). \tag{7}$$

Note, the solid velocity at the boundary, $V_s = \frac{\mathrm{d}h}{\mathrm{d}t} - \frac{\mathrm{d}h_m}{\mathrm{d}t}$, is the difference between the liquid layer growth rate and the melt rate. Substituting these vectors into the momentum balance and rearranging them we can determine an expression for the fluid velocity at $z = h$,

$$w|_{z=h} = \frac{\partial h}{\partial t} - \frac{\rho_s}{\rho_l} \frac{\partial h_m}{\partial t}. \tag{8}$$

To relate the pressure to the height of the liquid layer, h, a force balance is introduced

$$Mg - \int p \, dA = M \frac{dV_s}{dt}, \tag{9}$$

where A is the cross-sectional area of the base of the solid and gravity is denoted by g. The acceleration term, dV_s/dt, may be shown to be negligible, see [16]. Using the definition of the solid mass the force balance becomes,

$$4\rho_s LW[H_0 - h_m(t)]g = \int_{-L}^{L} \int_{-W}^{W} p dy dx \, . \tag{10}$$

The thermal problem is approximated by the following equations

$$T_{zz} = 0, \qquad \theta_t = \alpha_s \theta_{zz} \, , \tag{11}$$

where T, θ are the temperatures in the liquid and solid. The largest neglected term is $\mathcal{O}(\epsilon^2 Pe)$ where the Peclet number $Pe = U\mathcal{L}/\alpha_l$, and α_l is the thermal diffusivity. In the two-dimensional model of [16] it is shown that $\epsilon^2 Pe$ is the largest neglected term in the analysis ($\epsilon^2 Pe > \epsilon^2 Re > \epsilon^2$) and that it is negligible. Since we expect thinner films and so smaller values of ϵ this approximation will still be valid. A Stefan condition relates the height of the melted solid, h_m, to the heat flux across the boundary $z = h$,

$$\rho_s L_m \frac{dh_m}{dt} = k_s \left.\frac{\partial \theta}{\partial z}\right|_{z=h} - k_l \left.\frac{\partial T}{\partial z}\right|_{z=h}. \tag{12}$$

The thermal boundary conditions depend on which stage the melting process is in. During stage 1, $t \in [0, t_1]$, only conditions for the solid are needed. A cooling condition is prescribed at $z = 0$,

$$\left.\frac{\partial \theta}{\partial z}\right|_{z=0} = \frac{-q + h_{ss}(\theta|_{z=0} - T_0)}{k_s}, \tag{13}$$

where T_0 is the substrate temperature and h_{ss} is the heat transfer coefficient between the substrate and the solid. The block is insulated at the top, $z = h+H$,

$$\left.\frac{\partial \theta}{\partial z}\right|_{z=h+H} = 0. \tag{14}$$

Note that a large heat transfer coefficient, $h_{ss} \to \infty$, is equivalent to dealing with a fixed temperature boundary condition. Since $T_0 > T_m$ this ensures immediate melting and $t_1 = 0$. A small value, $h_{ss} \to 0$, is equivalent to a constant flux $\theta_z = -q/k_s$. For generality we therefore use a Newton cooling condition since it covers all standard boundary conditions, although in §4 we set $q = 0$.

Stage 2 begins as liquid appears on the surface $z = 0$ and then boundary conditions are also required for the liquid. The cooling condition at $z = 0$ is now

$$\left.\frac{\partial T}{\partial z}\right|_{z=0} = \frac{-q + h_{sl}(T|_{z=0} - T_0)}{k_l}. \tag{15}$$

At the melt interface, $z = h$,

$$T = \theta = T_m. \tag{16}$$

On the top surface (14) still holds. Stage 3 has the same boundary conditions as stage 2, but now the temperature in the solid is above the initial temperature everywhere and this affects the analytical solution. This is discussed further in the following section.

3. Analysis

The liquid velocities in the x and y directions can be calculated from equation (1). With the boundary conditions (3) and (4) we find

$$u = \frac{p_x}{2\eta} z(z-h), \qquad v = \frac{p_y}{2\eta} z(z-h). \tag{17}$$

An equation for the pressure is found by integrating the incompressibility condition (2) across the height of the liquid layer $z \in [0, h]$, and applying (17) and (8) to obtain,

$$\frac{\partial h}{\partial t} - \frac{\rho_s}{\rho_l}\frac{\partial h_m}{\partial t} = \frac{h^3}{12\eta}\nabla^2 p. \tag{18}$$

Rearranging this we obtain a form of Poisson's equation,

$$\nabla^2 p = \frac{12\eta}{h^3}\left(\frac{\partial h}{\partial t} - \frac{\rho_s}{\rho_l}\frac{\partial h_m}{\partial t}\right) = f(t)\,. \tag{19}$$

Applying the ambient pressure boundary conditions, the pressure equation may be solved via the following eigenfunction expansion,

$$p = \sum_{n=1}^{\infty} b_n(s,t)\sin(\omega_n r), \tag{20}$$

where we have shifted axes,

$$r = \frac{x+L}{2}, \qquad\qquad s = \frac{y+W}{2}\,. \tag{21}$$

Equation (19) becomes

$$\sum_{n=1}^{\infty}\left(\frac{\partial^2 b_n}{\partial s^2} - \omega_n^2 b_n\right)\sin(\omega_n r) = 4f(t), \tag{22}$$

where $\omega_n = n\pi/L$. Using the orthogonality condition the expression in brackets can be written as

$$\frac{\partial^2 b_n}{\partial s^2} - \omega_n^2 b_n \;=\; 4f(t)\frac{2}{L}\int_0^L \sin(\omega_n r)dr = 8f(t)\frac{1-(-1)^n}{n\pi}. \tag{23}$$

The boundary conditions at $y = \pm W$ indicate $b_n(0) = b_n(W) = 0$ and so we obtain

$$b_n(s,t) = 8f(t)\frac{1-(-1)^n}{n\omega_n^2\pi}\left[\frac{e^{-\omega_n s}(e^{\omega_n W}-1)}{e^{\omega_n W}-e^{-\omega_n W}} + \frac{e^{\omega_n s}(e^{-\omega_n W}-1)}{e^{-\omega_n W}-e^{\omega_n W}}\right]. \tag{24}$$

At the end of [16] the 3D extension to their model is briefly described, but not solved. The above expression for the coefficients b_n is different to that quoted in [16]. Equation (20), with the coefficients given by (24), is the formulation that provides the correct pressure distribution.

Substituting the expression for pressure into the force balance (10) we obtain,

$$4\rho_s LW[H_0 - h_m(t)]g = f(t)\Phi, \tag{25}$$

where,

$$\Phi = \sum_{n=1}^{\infty}\frac{32(1-(-1)^n)(-2e^{\omega_n W} + \omega_n W e^{\omega_n W} + 2 + \omega_n W)}{n\pi\omega_n^4(e^{\omega_n W}+1)}(\cos\omega_n L - 1)\,, \tag{26}$$

is a negative constant. As is often the case with this form of expansion, the terms decay rapidly so that only the initial terms are important. In the following we take only the first term of the series

$$\Phi \approx -\frac{128L^4}{\pi^5}\left[\frac{\pi W}{L} + 2\tanh\frac{\pi W}{L}\right]. \tag{27}$$

To verify the accuracy of this approximation we note that the two-dimensional limit is achieved by letting $W \to \infty$ so that $\Phi \to -128WL^3/\pi^4$. Comparison of the force balance (25) with the equivalent two-dimensional expression in [16] shows that the difference only occurs in the numerical coefficient $128/\pi^4 \approx 1.314$ as opposed to the two-dimensional value 1.33, *i.e.* an error of 1.2%. This is well within the errors generated through the approximations already made. Note, in the subsequent results section (where $W/L \approx 6$) we also compared results using (27) and taking 50 terms in (26) and found no visible difference.

Substituting $f(t)$ from equation (19) and rearranging (25) we obtain an equation involving the two unknown heights, h and h_m,

$$\frac{dh}{dt} = \frac{\rho_s g L W}{3\eta\Phi}h^3[H_0 - h_m] + \frac{\rho_s}{\rho_l}\frac{dh_m}{dt}. \tag{28}$$

To close the system this must be coupled to the Stefan condition (12). However, this involves the temperature gradients which are as yet unknown. Consequently we now analyse the thermal problem.

As discussed earlier the melting process may be split into three stages. Although the full problem is three-dimensional, due to the boundary conditions the thermal problem is one-dimensional and so the following thermal analysis is similar to that described in [16]. Consequently we will try to make the discussion brief and for further details refer the reader to [16]. The main difference between the current and the previous analysis lies in the use of the heat balance integral method (HBIM) to solve for the temperature in the solid. The HBIM involves choosing a function that approximates the temperature and then applying this function over a region which is determined through integrating the heat equation. The classical method uses a quadratic function [4, 9]. In [14], which describes the melting of a finite thickness solid, it is shown that a cubic approximating function is more accurate. This profile was then used in [16]. In the current paper we exploit a recent variation to the HBIM where the approximating function is chosen to minimise the error when the approximate temperature is substituted into the heat equation. This new method has been shown to significantly improve accuracy when studying problems with and without phase change, see [11, 12].

Stage 1. This is the pre-melt stage which simply involves solving the heat equation (11b) in the solid, subject to (13, 14). Provided the temperature rise above the initial temperature is negligible at the top of the block then the temperature

may be well approximated using the Laplace transform solution [3]:

$$\begin{aligned}\theta(z,t) &= \theta_0 + \frac{q - h_{ss}(\theta_0 - T_0)}{h_{ss}} \left[\operatorname{erfc}\left(\frac{z}{\sqrt{4\alpha_s t}}\right) \right. \\ &\left. -e^{h_{ss}z/k_s + \alpha_s t (h_{ss}/k_s)^2} \operatorname{erfc}\left(\frac{z}{\sqrt{4\alpha_s t}} + \frac{h_{ss}\sqrt{\alpha_s t}}{k_s}\right) \right] . \end{aligned} \tag{29}$$

In the melting stages, due to the presence of a moving boundary, we cannot use the Laplace transform solution consequently in [16] the HBIM was used. This a more versatile approximate solution, but usually suffers from a lack of accuracy. However, recently the method has been adapted to minimise errors and we will follow this new approach. Although unnecessary in stage 1 we use this method to demonstrate its accuracy before employing it in subsequent stages where no analytical verification is possible.

The HBIM starts by assuming an approximating function for the temperature, usually a polynomial of low order. The polynomial describes the temperature over a finite region where the temperature rise is non-negligible. This region is strictly defined by introducing an unknown length, known as the heat penetration depth $\delta(t)$, such that $\theta(\delta, t) = \theta_0$ and to ensure a smooth transition to the constant far-field temperature $\theta_z(\delta, t) = 0$. Applying these boundary conditions and the cooling condition at $z = 0$ we obtain

$$\theta(z,t) = \theta_0 + \frac{\delta(q + h_{ss}(T_0 - \theta_0))}{mk_s + \delta h_{ss}} \left(1 - \frac{z}{\delta}\right)^m . \tag{30}$$

The standard HBIM [4] uses an exponent $m = 2$, the value $m = 3$ was used in [16]. This choice was guided by the small argument expansion of the exact solution in stage 1. Following the work of [11] we will take the value $m = 3.584$ which has been shown to minimise the error in the temperature profile, based on a least-squares test (Fig. 5 in [11] indicates that at $t = 0.5$ the error is reduced by a factor of 6 by taking $m = 3.584$ rather than $m = 2$ and this difference increases for smaller times).

To determine $\delta(t)$ the HBIM proceeds by integrating the heat equation, with θ replaced by (30), over the region $z \in [0, \delta]$ to give a first order ordinary differential equation. Applying the initial condition $\delta(0) = 0$ the implicit solution to this equation is

$$t = \frac{1}{\alpha_s m(m+1)} \left[\frac{\delta^2}{2} + \frac{mk_s\delta}{h_{ss}} - \frac{m^2k_s^2}{h_{ss}^2} \ln\left(\frac{mk_s + \delta h_{ss}}{mk_s}\right) \right] . \tag{31}$$

Melting begins when the hottest part of the solid, obviously the part in contact with the substrate $z = 0$, reaches the melt temperature. Setting $\theta(0, t_1) = T_m$ in (30) we find

$$\delta(t_1) = \delta_1 = \frac{mk_s(T_m - \theta_0)}{q + h_{ss}(T_0 - T_m)}. \tag{32}$$

This provides the initial condition for δ in stage 2. The time t_1 when this occurs is obtained by substituting δ_1 into (31).

Stage 2. In stage 2 we must solve heat equations in the solid and liquid regions. Since the liquid layer is thin it is sufficient to deal with the linear profile determined from equation (11a), in the solid we still solve the full heat equation (11b). The boundary conditions are (14-16). The temperature in the liquid is then

$$T(z,t) = T_m - \frac{q + h_{sl}(T_0 - T_m)}{k_l + hh_{sl}}(z-h). \tag{33}$$

In the solid the HBIM requires the additional conditions $\theta(\delta,t) = \theta_0$ and $\theta_z(\delta,t) = 0$. The temperature profile is then

$$\theta(z,t) = \theta_0 + \frac{T_m - \theta_0}{\left(1 - \frac{h}{\delta}\right)^n}\left(1 - \frac{z}{\delta}\right)^n. \tag{34}$$

Since the base of the solid is now at a fixed temperature $\theta(h,t) = T_m$ the exponent $n = 2.235$ minimises the error [12]. Integrating the heat equation across the solid, $z \in [h,\delta]$ we find an equation involving the unknowns h, δ,

$$n\frac{dh}{dt} + \frac{d\delta}{dt} = \frac{\alpha_s n(n+1)}{\delta - h}. \tag{35}$$

Substituting for the temperature gradients in the Stefan condition, (12), provides an equation involving the third unknown h_m,

$$\rho_s L_m \frac{dh_m}{dt} = \frac{k_s n(\theta_0 - T_m)}{\delta - h} + \frac{k_l(q + h_{sl}(T_0 - T_m))}{k_l + hh_{sl}}. \tag{36}$$

The final equation required to close the system is the force balance (28) and then the system of three equations must be solved numerically, subject to initial conditions $\delta(t_1) = \delta_1$, $h(t_1) = h_m(t_1) = 0$. The solution is continued until the heat has penetrated through the entire solid, i.e. $\delta = h + H$, which then determines the time t_2. The values $h(t_2) = h_2$ and $h_m(t_2) = h_{m2}$ are then saved as initial conditions for stage 3.

Stage 3. In this final stage the entire solid has a temperature above the initial θ_0 and so it makes no sense to define a heat penetration depth, instead we have a new unknown which is the temperature at the top of the block. Since the top is insulated we impose $\theta_z(H+h,t) = 0$ and $\theta = \theta_H(t)$ (where θ_H is unknown). At the bottom we retain $\theta(h,t) = T_m$ and then the temperature may be expressed as

$$\theta(z,t) = \theta_H + \frac{T_m - \theta_H}{\left(1 - \frac{h}{h+H}\right)^n}\left(1 - \frac{z}{h+H}\right)^n, \tag{37}$$

where again $n = 2.235$.

Carrying through a standard heat balance integral leads to a complicated equation for θ_H. To simply this type of problem Goodman [4] proposed a function, ϕ, defined as the integral of the temperature over the domain of interest,

$$\phi = \int_h^{h+H} \theta dz = \frac{H}{4}(T_m + 3\theta_H). \tag{38}$$

This may be rearranged to give

$$\theta_H = \frac{1}{3}\left(\frac{4\phi}{H} - T_m\right). \tag{39}$$

Now integrating the heat equation over the solid $z \in [h, h+H]$ leads to an equation to determine ϕ:

$$\frac{d\phi}{dt} = \frac{3k_s(T_m - \theta_H)}{H_0 - h_m} + \theta_H\left(\frac{dh}{dt} - \frac{dh_m}{dt}\right) - T_m\frac{dh}{dt}, \tag{40}$$

where we may replace θ_H using (39).

Again the problem has been reduced to solving three first order differential equations, namely (40), the force balance (28) and the Stefan condition

$$\rho_s L_m \frac{dh_m}{dt} = \frac{k_s n(\theta_H - T_m)}{H_0 - h_m} + \frac{k_l(q + h_{sl}(T_0 - T_m))}{k_l + hh_{sl}}. \tag{41}$$

Continuity of temperature determines the initial condition for $\theta_H(t_2) = \theta_0$ and so $\phi(t_2)$, whilst $h(t_2) = h_2$, $h_m(t_2) = h_{m2}$. This system is solved until $h_m = H_0$ and melting is complete.

3.1. **Approximate analytical models.** We now consider a 'quasi-steady' model, equivalent to standard two-dimensional approximations, which will later be compared with the solution to the full problem. The solution is termed quasi-steady since it involves assuming that the melt layer thickness is constant, *i.e.* $h_t = 0$ (although h_m still varies with time). It also requires an isothermal, fixed mass solid, $h_m \ll H_0$. Under these assumptions the force balance and Stefan condition, equations (28), (41), may be written as

$$\frac{dh_m}{dt} = -\frac{\rho_l g LW}{3\eta\Phi}h^3 H_0 = \frac{k_l(q + h_{sl}(T_0 - T_m))}{\rho_s L_m(k_l + hh_{sl})}. \tag{42}$$

Since the quasi-steady height $h = h_q$ is constant we may determine the quasi-steady melt height by integrating the first two components of equation (42)

$$h_{mq} = -\frac{\rho_l g LW}{3\eta\Phi}h_q^3 H_0 t. \tag{43}$$

While h_q satisfies a quartic

$$3\eta\Phi\left[k_l(q + h_{sl}(T_0 - T_m))\right] + \left[\rho_s L_m(k_l + h_q h_{sl})\right]\rho_l g LW h_q^3 H_0 = 0, \tag{44}$$

determined by the second two components of (42).

In the limit $h_{sl} \to \infty$, that is we have a fixed temperature boundary condition, we reproduce a dimensional form of the first expression of Yoo [18]

$$h_q = \sqrt[4]{-\frac{3\eta\Phi k_l(T_0 - T_m)}{\rho_l \rho_s g L W H_0 L_m}}. \tag{45}$$

In the limit $h_{sl}h \ll k_l$ we find

$$h_q = \sqrt[3]{-\frac{3\eta\Phi(q + h_{sl}(T_0 - T_m))}{\rho_l \rho_s g L W H_0 L_m}} \tag{46}$$

and if we set $h_{sl} = 0$ we find a dimensional form of the second expression quoted in Yoo [18].

Yoo also studied a more complex model where h is allowed to vary but the change in mass and temperature variation in the solid are neglected. For a fixed temperature boundary condition the system then reduces to

$$\frac{dh}{dt} = \frac{\rho_s g L W}{3\eta\Phi} h^3 H_0 + \frac{\rho_s}{\rho_l}\frac{dh_m}{dt} \qquad \rho_s L_m \frac{dh_m}{dt} = \frac{k_l(T_0 - T_m)}{h}. \tag{47}$$

Eliminating h_m between the two equations leads to a single equation for h of the form

$$\frac{\partial h}{\partial t} = \frac{B}{h} - Ah^3 \tag{48}$$

where A, B are positive constants. Imposing $h(0) = 0$ (there is no stage 1 in this model) we find

$$h = \left[\sqrt{\frac{B}{A}} \tanh\left(2\sqrt{AB}\, t\right)\right]^{1/2}. \tag{49}$$

We may subsequently integrate (47b) to determine h_m, but the expression is rather complex so we leave it as an exercise for the reader.

4. Results

In the following we present results related to the experimental study of Moallemi *et al* [10]. Their work involved placing a block of n-octadecane initially at temperature 298K on a substrate at 308.2K. The melting temperature of n-octadecane is 301K. The sides and top of the block were well insulated and so melting primarily occurred at the bottom. Appropriate parameter values are given in Table 1.

The experimental investigation did not include a heat source at the substrate, so we set $q = 0$. This leaves us with one unknown parameter in each stage of melting: the heat transfer coefficient. During the latter two stages this parameter is key to predicting the correct melting time. During the initial stage, which lasts for a very short period it is not so important. In fact it is possible to neglect stage 1 and still obtain a good fit against the data. In the following we will include

Table 1: Parameter values for liquid/solid n-octadecane, see [10]

k_l	0.15	W m^{-1} K^{-1}	k_s	0.38	W m^{-1} K^{-1}
ρ_l	771.2	kg m^{-3}	ρ_s	930	kg m^{-3}
α_l	9.0×10^{-8}	m^2 s^{-1}	α_s	1.9×10^{-7}	m^2 s^{-1}
T_0	308.18	K	T_m	301.33	K
θ_0	298	K	L_m	2.435×10^5	J kg^{-1}
η	0.0036	N s m^{-2}	h_{sl}	3275	W m^{-2} K^{-1}
L	0.019	m	W	0.115	m
H_0	0.055	m			

stage 1, even though we have no way to calculate h_{ss}, since this makes the initial solutions smoother and also this is the only stage where we have an analytical check on the HBIM solution. To overcome the problem of not knowing the heat transfer coefficient in stage 1 we will set $h_{ss} = h_{sl}$.

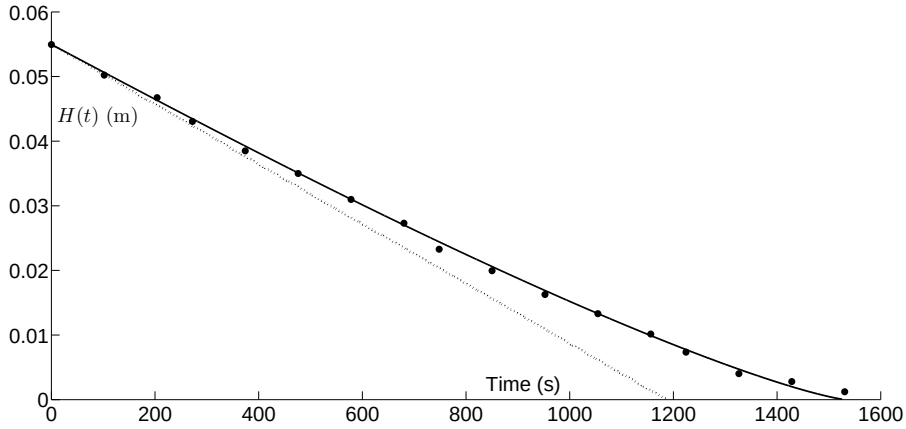

FIGURE 2. *The experimental data (circles) of $H(t)$ is compared to that of the 3D model with $h_{sl} = 3275W/m^2$ (solid line) and the quasi-steady solution (dotted line).*

Fig 2 shows a comparison of the experimental data (circles) reported in [10] with the current model (solid line). Clearly, the agreement between the current model and experiment is excellent. To obtain such a close fit we set $h_{sl} = 3275\text{W/m}^2$. Note, this is the only parameter we are free to choose. In a related problem of a droplet evaporating on a hot substrate [15] comparison with steady-state experiments permitted an accurate calculation of the heat transfer coefficient. This choice of HTC was then applied to other experiments to give

excellent results. An incorrect choice of HTC resulted in poor prediction of melting times and also gave an incorrect small time liquid height which affected the subsequent calculations. So, although in this study we only have one experimental data set with which to compare, the results of [15] give us confidence that our choice of HTC is correct. The third curve (dotted) shown on the figure is the quasi-steady solution of equation (43). The quasi-steady solution is accurate during the initial stages, consistent with the requirement that $h_m \ll H_0$, but as h_m increases it overpredicts the melting rate. This is an obvious consequence of setting $H = H_0$ for all time. Since it is the weight of the solid that causes the fluid flow and the weight is proportional to $H_0 - h_m$ neglecting h_m will impose a greater weight on the fluid than in reality. Setting $h_m = 0$ leads to a thinner fluid layer and faster melting. In Fig. 2 the full solution shows the process finishing at $t_m = 1525.66$s while the quasi-steady solution is nearly 24% faster with $t_m = 1169.2$s. Yoo [18] suggests that the mass variation may be neglected unless the initial height of the block is small compared to the contact area. In [10] a criterion is given based on $H_0/L > 0.1$ and the inverse Stefan number $c_l(T_0 - T_m)/L_m < 0.1$. From Fig. 2 and the above discussion it seems clear that the key factor is simply the proportion of melted solid. For example, we may expect errors in the solid height prediction of greater than 10% when $h_m > H_0/2$.

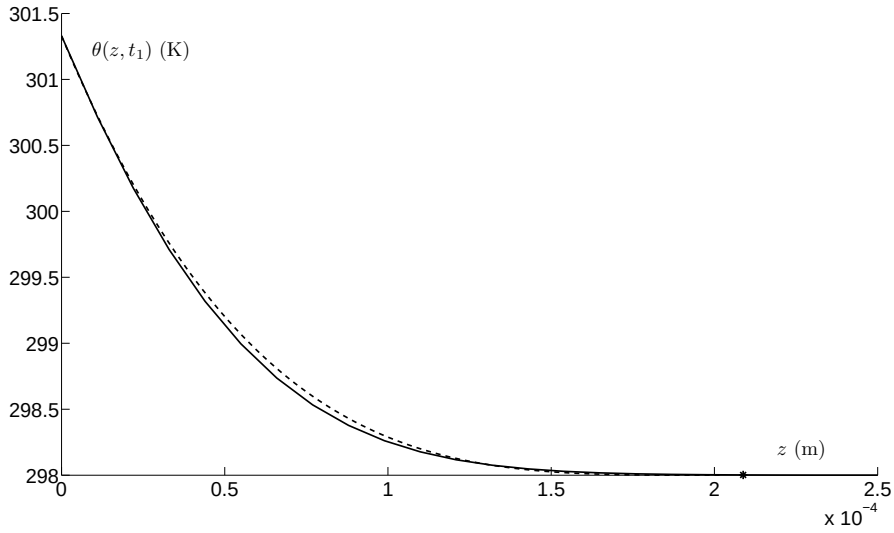

FIGURE 3. *The temperature in the solid at $t_1 s$ (at the end of stage 1). The solution from* (30) *(dashed line) is compared to the transform solution* (29) *(solid line), where the star denotes the penetration depth, $\delta_1 = 0.2mm$.*

The comparison with experimental data of Fig. 2 allowed us to accurately determine the heat transfer coefficient h_{sl}. With this knowledge we may now examine the whole process in more detail. During the first stage, before melting occurs, the temperature may be well approximated by the Laplace transform solution, equation (29). This also provides a check on the accuracy of the HBIM solution, equation (30). In Fig. 3 we compare the two solutions at time $t = t_1$, that is, just when melting is about to begin (using $h_{ss} = h_{sl}$). The value of t_1 for the two solutions may be found by setting $\theta(0, t) = T_m$ in equation (29) or from equations (31), (32) and using the parameter values of Table 1. The solid line is the transform solution and the dashed line the HBIM. The star denotes the position $x = \delta_1$, where the HBIM solution terminates. It is clear that the solutions are very close, with the only visible difference in the central region. The accuracy of the HBIM solution may also be inferred by the predicted values of t_1: the Laplace transform predicts $t_1 = 0.0113$s, the HBIM gives 0.0115s (a difference of less than 2%). Equation (32) gives the value of $\delta_1 \approx 0.2$mm which provides the initial condition for stage 2.

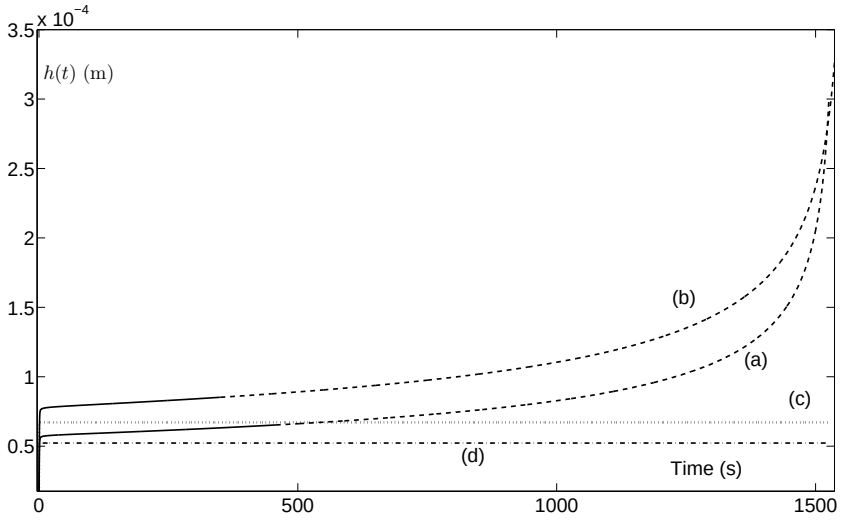

FIGURE 4. *Liquid height $h(t)$ for (a) 3D model with $h_{sl} = 3275\,W/m^2$, (b) 2D model with $h_{sl} = 7000\,W/m^2$, (c) 3D solution of* (49) *(d) quasi-steady solution. For curves (a), (b) stage 2 is the solid line, stage 3 is the dashed line.*

In Fig 4 the height of the liquid layer is plotted for both stages 2 and 3. The different sets of lines represent (a) the 3D model with $h_{sl} = 3275\text{W/m}^2$, (b) the 2D model of [16] with $h_{sl} = 7000\text{W/m}^2$, (c) the 3D solution of equation (49), (d) the quasi-steady solution, equation (44). Curves (a), (b) have two sections, stage 2 is the solid line, stage 3 is the dashed line. As predicted the liquid height for the 3D model is less than that for the 2D model. The quasi-steady solution

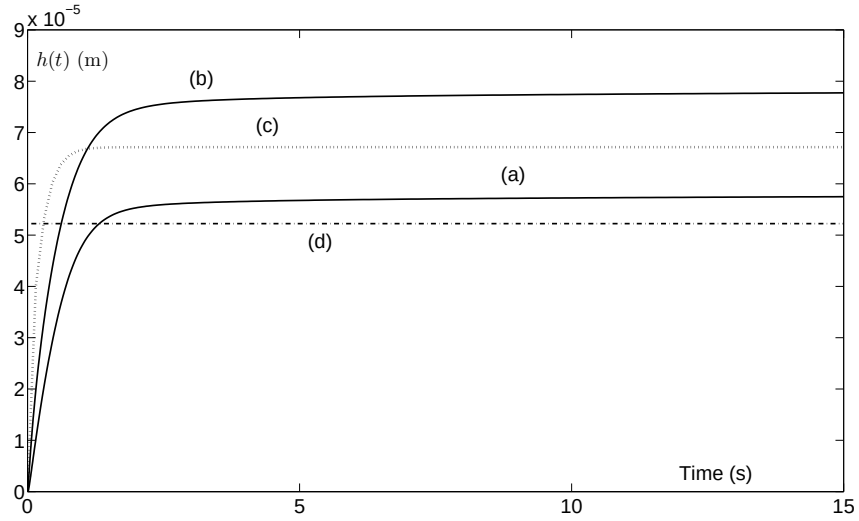

FIGURE 5. *Close up of initial stages of liquid height evolution. Curves as in Figure 4.*

has a constant height, h_q, which except for close to $t = 0$ lies well below the height predicted by the unsteady models (a) and (b). The two solutions (c) and (d) miss the final rise in $h(t)$ due to the neglect of h_m in the force balance. As $h_m \to H_0$ the weight of the solid tends to zero and so the solid is unable to squeeze out the water leading to a rapid increase in h. This increase in h also leads to a greater insulating effect which then slows down the melting. This manifests itself in the solution of Fig. 2 through the slow upward curve of $H(t)$. The analytical solution of equation (49) appears similar to the quasi-steady solution, in that it seems to take a constant (although higher) value. The higher value is a result of using an infinite heat transfer coefficient which then makes the height closer to that of the full solution. However, if we write down (47) with a finite HTC and then solve the equations numerically the curve levels off at the quasi-steady height shown by (d). So in fact the only difference between the quasi-steady solution and that of (47) is in the variation of h very close to $t = 0$. This may be seen more clearly in Fig. 5 which shows the evolution for the first 15s. Yoo discusses the time-scale for the unsteady period and suggests that for fixed temperature at $z = 0$ or constant flux the times are 11.4 and 8.5s respectively. We should stress that the analysis of Yoo should only be considered as a small time solution, valid for 10s of seconds, and should not be expected to apply over the whole melting process. Indeed, referring back to Fig.4 we can see that this 'transient period' is deceptive. Over the short time-scale shown on Fig. 5 the solutions all appear to level out. Over the longer time-scale of Fig. 4 it is clear that curves (a), (b) keep on increasing.

5. Simplified model

Judging from the results of Fig. 2 it is clear that we have a mathematical model that includes all important effects, such that we can accurately model the contact melting process. The question now is: can any of the model features be neglected to provide a simpler system whilst retaining the appropriate level of accuracy?

Inspection of the liquid height results in Figures 4 and 5 indicates that the quasi-steady solution significantly underpredicts the height and misses the initial transient in h completely. The more complex solution of equation (49), which results from the system (47), captures the initial transient but then asymptotes to a low constant value for h. Equations (47) require fixing the solid mass, neglecting heat transfer in the solid and using an infinite HTC. These factors are then our contenders for simplifying the system. If we take a finite HTC then the equivalent system to (47) involves two simple first order ODEs. The numerical solution of these equations has the same asymptote as the quasi-steady solution curve (d) while the initial transient retains a sharper gradient than that of curves (a), (b). In the initial stages of melting, as $t \to 0$, obviously $H \approx H_0$ and so the difference in gradients can only be a result of including the solid temperature.

To understand the contribution of the solid temperature we may compare its order of magnitude with that of the gradient in the liquid. A simple estimate indicates that in the solid $\theta_z \sim (\theta_0 - T_m)/H$, in the liquid $T_z \sim (T_0 - T_m)/h$ and so, if we take, for example, $\theta_0 - T_m = T_0 - T_m = 5$ then the ratio $\theta_z/T_z = h/H \approx 0.002 \ll 1$. From this we may conclude that the inclusion of θ_z in the model is unnecessary. However, the Stefan condition of stage 2, (36), gives us a more accurate picture of the temperature gradients. In particular at small times $t \approx t_1$ (and so $\delta \approx \delta_1$, $h \approx 0$) we see

$$\theta_z \approx \frac{n(\theta_0 - T_m)}{\delta} \approx 5 \times 10^4 \qquad T_z \approx \frac{h_{sl}(T_0 - T_m)}{k_l} \approx 10^5 \,. \tag{50}$$

So, in the early stages of melting, the temperature gradients are of the same magnitude: hence the difference in the gradient h_t at small times. However, for larger times $\theta_z \ll T_z$ and is therefore negligible. To summarise, if we wish to accurately model the early stages of melting then we must include the solid temperature. On the other hand, if we are willing to miss the detailed features of the initial melting it is reasonable to neglect the solid temperature.

Following this argument, for large times, when we deduce that the difference between the liquid heights for the full and quasi-steady model must then be attributed to the changing mass. Consequently, we propose that the contact melting process may be described by only two equations:

$$\frac{dh}{dt} = \frac{\rho_s g L W}{3\eta\Phi} h^3 [H_0 - h_m] + \frac{\rho_s}{\rho_l} \frac{dh_m}{dt} \tag{51}$$

$$\rho_s L_m \frac{dh_m}{dt} = \frac{k_l (q + h_{sl}(T_0 - T_m))}{k_l + h h_{sl}} \,, \tag{52}$$

subject to $h(0) = h_m(0) = 0$. For a given material these equations demonstrate that contact melting is controlled by the solid dimensions L, W, H_0, the heat transfer coefficient and the substrate temperature. The solid temperature does not enter the system. Note, although these equations are significantly simpler than the full model we still cannot obtain an analytical solution. Further, we solved the full model using MATLAB routine ODE45. Due to the neglect of the temperature gradient in the solid the simpler system has an initial very rapid fluid layer growth. This requires us to use ODE15s, which is for stiff systems.

5.1. **Linear melting model.** In the introduction we stated that the thickness of melted material is proportional to time. From Fig. 2 we see that the H solution actually curves slowly upwards as time progresses, that is, $|H_t|$ is a slowly decreasing function of time. Since $H = H_0 - h_m$ we can then infer that dh_m/dt also varies only slowly with time. As a simple approximation we may then look for a solution of the form $h_m = \alpha t$. Assuming α to be constant it is sufficient to find its value at any time and then we have an explicit expression for h_m. At the beginning of stage 2 we know that $h = 0, \delta = \delta_1$ and so the Stefan condition (36) may be written

$$\frac{dh_m}{dt} = \frac{1}{\rho_s L_m}\left[\frac{k_s n(\theta_0 - T_m)}{\delta_1} + h_{sl}(T_0 - T_m))\right]. \tag{53}$$

Using the definition of δ_1 and the numerical values of n, m this simplifies to

$$\frac{dh_m}{dt} = \frac{h_{sl}(T_0 - T_m)}{\rho_s L_m}\left[1 - \frac{n}{m}\right] = 0.376\,\frac{h_{sl}(T_0 - T_m)}{\rho_s L_m} = \alpha\,. \tag{54}$$

Taking the values of Table 1 we find $\alpha \approx 3.73 \times 10^{-5}$m/s. Since $H \approx H_0 - \alpha t$, melting is complete when $t = t_m = H_0/\alpha \approx 1507$s. The value from the full solution is $t_m = 1526$s, so the approximate solution is very close (1.2% faster).

A remarkable feature of this analytical solution is the (seemingly impossible) lack of parameters. With the assumption that α is constant we are free to calculate it at any time. By choosing the time t_1, just when the liquid appears, we avoid many of the complications of the analysis such as the weight of the solid and the initial temperature. From equation (54) we may then deduce that the key parameters, for a given material, are simply the substrate temperature and HTC. The numerical coefficient $1 - n/m = 0.376$ is an important parameter, indicating the importance of using an accurate HBIM.

In Fig. 6 we compare the experimental data (circles), the full three-dimensional solution (solid line), the solution of equations (51,52) (dashed line) and the linear melt model $H(t) = H_0 - \alpha t$ (dotted). Clearly the two equation model shows excellent agreement with the data and, provided ones interest does not lie in the details of initial melting, it would therefore seem sensible in general to use (51,52) to describe the contact melting process. The linear melt model is not so close during most of the process but captures, possibly fortuitously, the melt time quite

well. It would be very interesting to compare it with other experimental results.

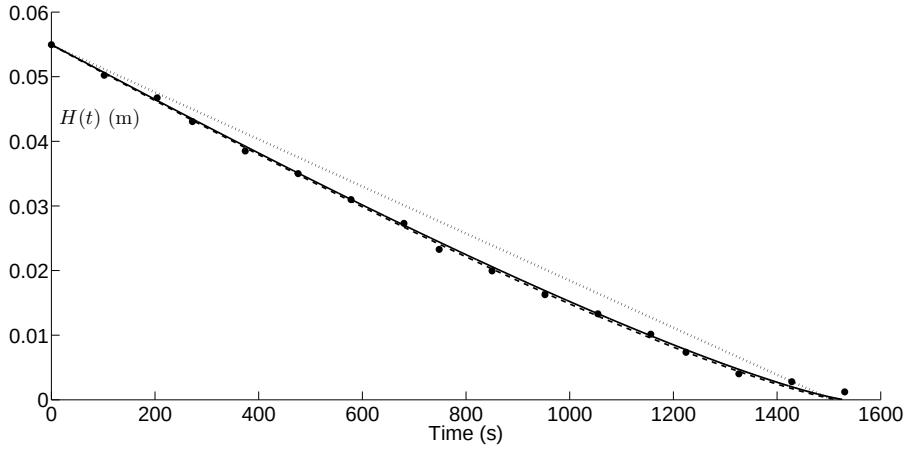

FIGURE 6. *Comparison of experimental data (circles), full model (solid line), approximate model of equations (50, 52)(dashed line) and linear melting model* $h_m = \alpha t$ *(dotted)*

6. Conclusions

In this paper a model for a three-dimensional contact melting process has been presented. The work is an extension of the two-dimensional study of [16] where the governing equations were reduced systematically, meaning that the terms neglected in the approximate solution are indeed negligible. As a result, our model reduced to solving three first order ordinary differential equations and the results showed excellent agreement when compared to experimental data. As expected the three-dimensional model requires a lower HTC than the two-dimensional model, although only by a factor of 2. This may be attributed to the fact that in the experiments a relatively large aspect ratio was used, $W/L = 6$. Reducing this value should increase the difference between two and three dimensional models.

A number of more approximate solutions were also studied. The standard 'quasi-steady' approximation, which requires constant temperature and mass of the solid and a constant fluid layer thickness, leads to a fluid thickness of the correct order of magnitude but (except for in the vicinity of $t = 0$) lower than the actual value and the discrepancy increases with time. A slightly more complex model, allowing h to vary whilst neglecting the solid mass and temperature variation merely smoothes the initial jump in h but the final value is still the same as predicted by the quasi-steady model. Neglecting the solid temperature variation means that gradient h_t is still higher than that predicted by the full model. Both models miss the final sharp rise in liquid height.

Careful analysis of the results and equations showed that the main culprit in the inaccuracy of existing approximate models was due to neglect of the solid mass variation. Provided the details of the initial melting process are not of primary interest, it was shown that three-dimensional contact melting on a flat substrate may be well described by two first order ordinary differential equations. These indicate that for a given material melting is controlled by the solid dimensions, substrate temperature and heat transfer coefficient. Interestingly, the initial solid temperature does not affect the melting (it's importance is limited to the initial stages).

Finally we noted that the decrease in solid height was approximately linear and then used this to determine a simple formula for the melt time. This indicated that the controlling parameters were simply the HTC and substrate temperature, other parameters appear to be of secondary importance. However, we would need more experimental data to be confident of this conclusion.

Acknowledgments

MDD gratefully acknowledges the support of a PhD grant from the Centre de Recerca Matemática. TM gratefully acknowledges the support of this research through the Marie Curie International Reintegration Grant *Industrial applications of moving boundary problems*, grant no. FP7 - 256417, Ministerio de Ciencia e Innovación grant MTM2010-17162 and partial support by the project 2009-SGR-345 from AGAUR-Generalitat de Catalunya.

References

[1] C. Clanet A. L. Biance and D. G. Quere. Leidenfrost drops. *Phys. Fluids*, 14:1632, 2003.
[2] A. Bejan. Contact melting heat transfer and lubrication. *Adv. Heat Transfer*, 24, 1994.
[3] H. S. Carslaw and J. C. Jaeger. *Conduction of Heat in Solids, 2nd Edition*. Oxford University Press, London, 1959.
[4] T. R. Goodman. The Heat-Balance Integral and Its Application to Problems Involving a Change of Phase. *Trans. ASME*, 80: 335–342, 1958.
[5] D. Groulx and M. Lacroix. Study of close contact melting of ice from a sliding heated flat plate. *Int. J. Heat Mass Trans.*, 19:4407 – 4416, 2006.
[6] S. Okawa H. Kumano, A. Saito and Y. Yamada. Study of direct contact melting with hydrocarbon mixtures as the PCM. *Int. J. Heat Mass Trans.*, 48(15):3212–3220, 2005.
[7] H. Hong H. Yoo and C. Kim. Effects of transverse convection and solid-liquid density difference on the steady close-contact melting. *International Journal of Heat and Fluid Flow*, 19:368–373, 1998.
[8] M. Lacroix. Contact melting of a phase change material inside a heated parallelepedic capsule. *Energy Conversion and Management*, 42:35 – 47, 2001.
[9] S. L. Mitchell and T. G. Myers. Application of standard and refined heat balance integral methods to one-dimensional Stefan problems. *SIAM Review*, 52(1):57–86, 2010. DOI. 10.1137/080733036.
[10] M.K. Moallemi, B.W. Webb, and R. Viskanta. An experimental and analytical study of close-contact melting. *Int. J. Heat Trans.*, 108:894 – 899, 1986.

[11] T. G. Myers. Optimizing the exponent in the heat balance and refined integral methods. *Int. Comm. Heat Mass Trans.*, 36(2):143–147, 2009, DOI:10.1016/j.icheatmasstransfer.2008.10.013.

[12] T. G. Myers. Optimal exponent heat balance and refined integral methods applied to Stefan problems. *Int. J. Heat Mass Trans.*, 53, 2010 DOI:10.1016/j.ijheatmasstransfer.2009.10.045.

[13] T. G. Myers, J.P.F. Charpin, and C.P. Thompson. Slowly accreting ice due to supercooled water impacting on a cold surface. *Phys. Fluids*, 14(1):240 – 256, 2002.

[14] T. G. Myers, S. L. Mitchell, G. Muchatibaya, and M. Y. Myers. A cubic heat balance integral method for one-dimensional melting of a finite thickness layer. *Int. J. Heat & Mass Trans.*, 50: 5305–5317, 2007.

[15] T.G. Myers and J.P.F. Charpin. A mathematical model of the Leidenfrost effect on an axisymmetric droplet. *Phys. Fluids*, 21, 063101, 2009 DOI: 10.1063/1.3155185.

[16] T.G. Myers, S.L. Mitchell, and G. Muchatibaya. Unsteady contact melting of a rectangular cross-section phase change material on a flat plate. *Phys. Fluids*, 20 103101, 2008 DOI:10.1063/1.2990751.

[17] H. Ockendon and J. R. Ockendon. *Viscous Flow*. Cambridge Texts in Applied Mathematics, 1995.

[18] H. Yoo. Analytical solutions to the unsteady close-contact melting on a flat plate. *Int. J. Heat Mass Trans.*, 3:1457 – 1467, 2000.

Tim G. Myers
Centre de Recerca Matemàtica
Campus de Bellaterra, Edifici C
08193 Bellaterra (Barcelona)
Spain
E-mail address: tmyers@crm.cat